

See discussions, stats, and author profiles for this publication at: <https://www.researchgate.net/publication/5261853>

# Artificial Ion Channel Biosensor in Human Immunodeficiency Virus gp41 Drug Sensing

ARTICLE in ANALYTICAL CHEMISTRY · AUGUST 2008

Impact Factor: 5.64 · DOI: 10.1021/ac800511n · Source: PubMed

CITATIONS

7

READS

28

## 2 AUTHORS:



Yanxia Hou

Institut nanosciences et Cryogénie, france

29 PUBLICATIONS 404 CITATIONS

SEE PROFILE



Miriam Gochin

Touro University College of Osteopathic M...

62 PUBLICATIONS 1,251 CITATIONS

SEE PROFILE

# Artificial Ion Channel Biosensor in Human Immunodeficiency Virus gp41 Drug Sensing

Yanxia Hou<sup>†,‡,§</sup> and Miriam Gochin<sup>\*†,‡</sup>

Department of Basic Sciences, Touro University-California, Vallejo, California 94592, and Department of Pharmaceutical Chemistry, University of California San Francisco, San Francisco, California 94143

An ion channel biosensor is described for label-free detection of inhibitors which bind to the coiled coil domain of human immunodeficiency virus type 1 gp41. gp41 is the viral transmembrane glycoprotein responsible for fusion between HIV-1 and host cells. The N-terminal coiled coil domain binds three antiparallel C-heptad repeat peptides in the six helix bundle structure of trimeric gp41 that forms during fusion. Compounds able to prevent six-helix bundle formation by binding to the gp41 coiled coil could inhibit fusion and have important therapeutic potential. We have immobilized on gold a positively charged metalloprotein mimic of a section of the gp41 coiled coil containing a hydrophobic pocket suitable for small molecule binding. We demonstrate that the resulting sensor is able to transmit a current in the presence of negatively charged redox marker ions, therefore acting as an artificial ion channel. The electrochemical signal, measured by cyclic voltammetry, was modulated by specific analyte binding to the coiled coil. Nanomolar quantities of peptides and small molecules that bind in the hydrophobic pocket could be selectively detected, providing a method for label-free detection of binding to gp41.

Biosensors have been widely applied in various fields for analyte detection due to their simplicity, high sensitivity, and potential ability for real-time and on-site analysis. The typical biosensor is tailored for detection of a specific analyte, often using optical or electrochemical transduction systems.<sup>1–3</sup> Application of biosensors in the pharmaceutical arena is growing<sup>4,5</sup> with the goal of achieving high-throughput screening of combinatorial libraries for label-free detection of new drugs. A biosensor for this application should be able to discriminate between multiple analytes, ideally ranking them by binding affinity.

In this paper we demonstrate an artificial ion channel biosensor for specific detection of inhibitors that bind to the N-terminal

coiled coil domain of the glycoprotein gp41 of human immunodeficiency virus type 1 (HIV-1). The gp41 coiled coil is an important target for entry inhibitors that are able to prevent fusion of viral and host cell membranes.<sup>6</sup> During fusion, a conformational rearrangement of gp41 exposes the trimeric coiled coil domain, prior to the formation of a six-helix bundle (6-HB) with three antiparallel C-terminal helices of gp41.<sup>7–9</sup> The existing approved drug against HIV fusion is a peptide derived from the C-terminal helix and pretransmembrane region, Enfuvirtide (T20), which has high potency but poor bioavailability.<sup>10</sup> Methods to identify low-molecular weight fusion inhibitors include screening for compounds that bind to the coiled coil domain, potentially inhibiting six-helix bundle formation.<sup>11–14</sup> Current screening methods include cell-based fusion and infectivity assays,<sup>15,16</sup> an ELISA assay for the 6-HB<sup>14</sup> and fluorescence intensity<sup>17</sup> or polarization<sup>18</sup> assays that are able to quantitatively detect peptide binding, and small molecule binding by competitive inhibition.

We describe the development of an artificial ion channel sensor for label-free direct detection of binding to gp41. Artificial ion channel sensors (ICS) consist of an electrode surface modified with a layer of charged biological or synthetic material and respond to oppositely charged redox marker ions, generating a current when the marker ions are oxidized or reduced at the electrode.<sup>19–21</sup> The current is caused by electron shuttling through pores in the immobilized layer<sup>21</sup> and can be modulated by

- (6) Debnath, A. K. *Curr. Opin. Investig. Drugs* **2006**, *7*, 118–27.
- (7) Chan, D. C.; Fass, D.; Berger, J. M.; Kim, P. S. *Cell* **1997**, *89*, 263–73.
- (8) Gallo, S. A.; Puri, A.; Blumenthal, R. *Biochemistry* **2001**, *40*, 12231–6.
- (9) Melikyan, G. B.; Markosyan, R. M.; Hemmati, H.; Delmedico, M. K.; Lambert, D. M.; Cohen, F. S. *J. Cell. Biol.* **2000**, *151*, 413–23.
- (10) Manfredi, R.; Sabbatani, S. *Curr. Med. Chem.* **2006**, *13*, 2369–84.
- (11) Kilgore, N. R.; Salzwedel, K.; Reddick, M.; Allaway, G. P.; Wild, C. T. *J. Virol.* **2003**, *77*, 7669–72.
- (12) Root, M.; Steger, H. *Curr. Pharm. Design* **2004**, *10*, 1805–25.
- (13) Wild, C. T.; Shugars, D. C.; Greenwell, T. K.; McDaniel, C. B.; Matthews, T. J. *Proc. Natl. Acad. Sci. U.S.A.* **1994**, *91*, 9770–4.
- (14) Jiang, S.; Lin, K.; Zhang, L.; Debnath, A. K. *J. Virol. Methods* **1999**, *80*, 85–96.
- (15) Ji, C.; Zhang, J.; Cammack, N.; Sankuratri, S. *J. Biomol. Screen.* **2006**, *11*, 65–74.
- (16) Bradley, J.; Gill, J.; Bertelli, F.; Letafat, S.; Corbau, R.; Hayter, P.; Harrison, P.; Tee, A.; Keighley, W.; Perros, M.; Ciaramella, G.; Sewing, A.; Williams, C. *J. Biomol. Screen.* **2004**, *9*, 516–24.
- (17) Cai, L.; Gochin, M. *Antimicrob. Agents Chemother.* **2007**, *51*, 2388–95.
- (18) Mo, H.; Konstantinidis, A. K.; Stewart, K.; Dekhtyar, T.; Ng, T.; Swift, K.; Matayoshi, E.; Kati, W.; Kohlbrenner, W.; Molla, A. *Virology* **2004**, *329*, 319–27.
- (19) Han, S.; Lin, J.; Satjapipat, M.; Baca, A. J.; Zhou, F. *Chem. Commun.* **2001**, 609–10.
- (20) Umezawa, Y.; Aoki, H. *Anal. Chem.* **2004**, *76*, 321A–6A.
- (21) Schon, P.; Degefa, T. H.; Asaftei, S.; Meyer, W.; Walder, L. *J. Am. Chem. Soc.* **2005**, *127*, 11486–96.

\* To whom correspondence should be addressed. E-mail: mgochin@touro.edu.

<sup>†</sup> Touro University-California.

<sup>‡</sup> University of California San Francisco.

<sup>§</sup> Current address: Département des Microtechnologies pour la Biologie et la Santé (DTBS), Laboratoire d'électronique et de technologies de l'information (LETI), Commissariat à l'Énergie Atomique (CEA), 17 Rue Des Martyrs, 38054 Grenoble, France.

- (1) Cooper, M. A. *Drug Discovery Today* **2006**, *11*, 1068–74.
- (2) Cretich, M.; Damin, F.; Pirri, G.; Chiari, M. *Biomol. Eng.* **2006**, *23*, 77–8.
- (3) Homola, J.; Yee, S. S.; Gauglitz, G. *Sens. Actuators, B* **1999**, *54*, 3–15.
- (4) Keusgen, M. *Naturwissenschaften* **2002**, *89*, 433–44.
- (5) Meadows, D. *Adv. Drug Delivery Rev.* **1996**, *21*, 179–89.

interaction of the layer with a specific analyte.<sup>22–25</sup> Few examples exist of ion channel sensors for protein–protein or protein–small molecule interaction studies<sup>21,23,25,26</sup> and none to our knowledge in which detection of more than one specific analyte was demonstrated.

We constructed an ICS using a charged gp41 coiled coil complex stabilized by octahedral Fe<sup>2+</sup> coordination to bipyridyl groups at the N-termini of component peptides. A similar construct has been utilized for fluorescence screening to detect small molecule fusion inhibitors binding to the coiled coil.<sup>17</sup> It contains the residues of a hydrophobic pocket identified as a target for drug binding.<sup>27</sup> We demonstrate use of the ICS for electrochemical detection of peptide and small molecule binding. An equivalent biosensor was elaborated and examined using surface plasmon resonance (SPR) to confirm the electrochemical findings. Both SPR and electrochemical experiments facilitated direct detection of gp41 inhibitors, with the electrochemical experiment having the possibility of much lower instrument cost and relative insensitivity to analyte molecular weight.

## MATERIALS AND METHODS

**Reagents.** Unless otherwise indicated, chemicals were ordered from Sigma-Aldrich (St. Louis, MO) and used without further purification. Peptides were prepared by solid phase synthesis (Biosynthesis, Inc., Texas). 2,2'-Bipyridine-5'-carboxylate (bpy) was prepared according to literature methods<sup>28</sup> and attached to the N-terminus of coiled coil peptides on the resin. The Fe<sup>II</sup> complex of bipyridylated peptides was prepared by addition of 1/3 stoichiometry of freshly prepared ferrous ammonium sulfate to peptide in 25 mM Tris-acetate buffer at pH 7.0.

**Instrumentation.** Electrochemical measurements were performed on an electrochemical quartz crystal microbalance (EQCM 400A, CH Instruments, Texas) in a conventional three-electrode cell, with a 0.2 cm<sup>2</sup> Au surface of a 0.51 cm diameter quartz crystal as the working electrode, Pt wire as the counter electrode, and Ag/AgCl (3 M KCl) as the reference electrode. Cyclic voltammetry (CV) was carried out in 2 mL of 25 mM Tris-acetate buffer solution (100 mM NaCl, pH 7.0) in the presence of the redox probe consisting of 2 mM K<sub>3</sub>Fe(CN)<sub>6</sub> and 2 mM K<sub>4</sub>Fe(CN)<sub>6</sub>. The potential was swept between 0–0.5 V at a rate of 100 mV s<sup>-1</sup>. Before each CV measurement, N<sub>2</sub> flow was introduced to remove O<sub>2</sub> in the solution. Surface plasmon resonance measurements were performed on a Biacore 1000 (Biacore, Sweden) using a carboxymethylated dextran-coated CM5 chip for surface modification.

**Sensor Surface Preparation for Cyclic Voltammetry.** Before use, the Au coated quartz crystal was cleaned with acetone for 5 min in an ultrasonic bath, dried under N<sub>2</sub>, and then immersed into freshly prepared hot piranha solution (H<sub>2</sub>SO<sub>4</sub>/H<sub>2</sub>O<sub>2</sub> = 7/3 v/v)

for 1–2 min, followed by thorough cleaning with ethanol for 15 min, and drying under N<sub>2</sub>. The crystal was functionalized with mixed self-assembled monolayers (SAMs) of 11-mercaptopundecanoic acid and 6-mercapto-1-hexanol (1:1) by exposure to 1 mM of each alkanethiol for 20 h. The peptide ligand was covalently immobilized through the carboxylate groups by using a standard ligand–thiol coupling procedure according to a Biacore application note (<http://www.sprpages.nl/Experiments/Thiol.htm>), as follows: The carboxylate groups were activated for 30 min with a solution of 5 mM *N*-(3-dimethylaminopropyl)-*N'*-ethylcarbodiimide hydrochloride (EDC) and 8 mM *N*-hydroxysulfosuccinimide (Pierce Chemicals) (NHS) (1:1 v/v) in 25 mM PBS buffer at pH 7.0. A reactive disulphide group was then introduced with a thiol coupling reagent 2-(2-pyridinyldithio)ethaneamine hydrochloride (PDEA) with a concentration of 80 mM in 0.1 M sodium borate buffer (pH 8.5) for 30 min. [Fe(envC)<sub>3</sub>]<sup>2+</sup> ligand was anchored on the surface by application of a 54 μM solution for 2 h at 4 °C. Excess unreacted disulfide groups were deactivated with 50 mM L-cysteine in 0.1 M sodium acetate, 1 M NaCl at pH 4.3 for 20 min. To counteract leaching of Fe<sup>2+</sup> from the anchored complex at low pH, a solution of 10 mM Fe(NH<sub>4</sub>)<sub>2</sub>(SO<sub>4</sub>)<sub>2</sub> in ultrapure water was introduced on the crystal surface for 10 min.

**Sensor Surface Preparation for SPR.** A similar tethering scheme was used on a CM5 carboxymethylated dextran-coated chip for SPR by following the Biacore thiol coupling protocol (<http://www.sprpages.nl/Experiments/Thiol.htm>) (See Supporting Information).

## RESULTS AND DISCUSSION

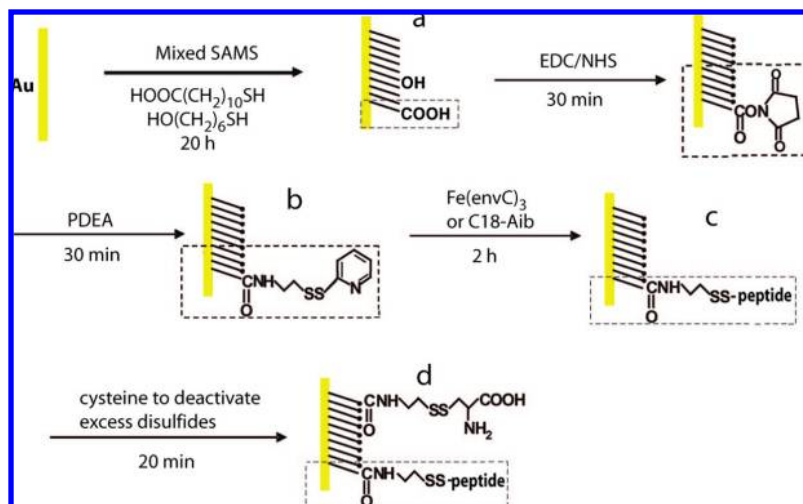
**Bioreceptor Selection.** A coiled coil complex was formed from the association of three equivalent gp41 N heptad repeat peptides stabilized by octahedral Fe<sup>2+</sup> coordination to bipyridyl (bpy) groups at the peptide N-termini. The resulting complex [Fe(envC)<sub>3</sub>]<sup>2+</sup> was used as a bioreceptor for sensor preparation. The sequence of envC is bpy-GQAVEAQQHLLQLTVWGIK-QLQARI-D-C-amide. Underlined residues occur in wild-type gp41, and the residues in bold define a hydrophobic pocket in the trimeric structure. [Fe(envC)<sub>3</sub>]<sup>2+</sup> contains D-cysteine (DC) at the C-terminal end in order to create a monolayer with vertical attachment of the coiled coil.<sup>29</sup> In addition, biosensors were prepared using the corresponding C heptad repeat peptide C18-Aib: Ac-WBEWDREIBNYTSLIC-amide, which binds to [Fe(envC)<sub>3</sub>]<sup>2+</sup> and to a slightly longer more soluble equivalent [Fe(env2.0)<sub>3</sub>]<sup>2+</sup>, where env2.0 has the sequence bpy-GQAVEAQQHLLQLTVWGIKQLQARILAVEKK-amide.<sup>17,30</sup> C18-Aib has two α-aminoisobutyric acid residues (B) which promote helical structure.<sup>31</sup> The N- and C-peptide constructs were used as test analytes on the opposing sensors.

**Layer-by-Layer Assembly of the Bioreceptor Monitored by CV.** The electrochemical biosensors were constructed using layer-by-layer assembly on a gold-plated quartz crystal, as depicted in Scheme 1. The steps in assembly consisted of formation of mixed self-assembled monolayers of alkanethiols (1:1 11-mercaptopundecanoic acid and 6-mercapto-1-hexanol).

- (22) Katayama, Y.; Ohuchi, Y.; Higashi, H.; Kudo, Y.; Maeda, M. *Anal. Chem.* **2000**, *72*, 4671–4.
- (23) Kuramitz, H.; Matsuda, M.; Thomas, J. H.; Sugawara, K.; Tanaka, S. *Analyst* **2003**, *128*, 182–6.
- (24) Bonanni, A.; Esplandi, M. J.; Pividori, M. I.; Alegret, S.; del Valle, M. *Anal. Bioanal. Chem.* **2006**, *385*, 1195–201.
- (25) Murata, M.; Nakayama, M.; Irie, H.; Yakabe, K.; Fukuma, K.; Katayama, Y.; Maeda, M. *Anal. Sci.* **2001**, *17*, 387–90.
- (26) Murata, M.; Gonda, H.; Yano, K.; Kuroki, S.; Suzutani, T.; Katayama, Y. *Bioorg. Med. Chem. Lett.* **2004**, *14*, 137–41.
- (27) Chan, D. C.; Chutkowski, C. T.; Kim, P. S. *Proc. Natl. Acad. Sci. U.S.A.* **1998**, *95*, 15613–7.
- (28) Huang, T. L. J.; Brewer, D. G. *Can. J. Chem.* **1981**, *59*, 1689–1700.

- (29) Case, M. A.; McLendon, G. L.; Hu, Y.; Vanderlick, T. K.; Scoles, G. *Nano Lett.* **2003**, *3*, 426–9.
- (30) Gochin, M.; Savage, R.; Hinckley, S.; Cai, L. *Biol. Chem.* **2006**, *387*, 477–83.
- (31) Sia, S. K.; Carr, P. A.; Cochran, A. G.; Malashkevich, V. N.; Kim, P. S. *Proc. Natl. Acad. Sci. U.S.A.* **2002**, *99*, 14664–9.

## Scheme 1. Layer-by-Layer Assembly of Bioreceptors on a Gold-Plated Quartz Crystal<sup>a</sup>



<sup>a</sup> The experimental CV traces corresponding to steps a–d upon immobilization of  $\text{Fe}(\text{envC})_3$  are shown in Figure 1.

canoic acid and 6-mercapto-1-hexanol) on gold, EDC/NHS activation of terminal carboxylate groups, PDEA coupling, and disulfide bond formation with the C-terminal cysteine of the peptide. The mercaptohexanol filler was used to reduce nonspecific hydrophobic protein binding to the surface<sup>32</sup> and reduce the density and steric hindrance of the bioreceptors, enabling access of analytes to the binding sites which are midway down the coiled coil. Surface activation was followed by a low pH cysteine wash, to deactivate any uncoupled PDEA on the surface while dislodging nonspecifically adsorbed hydrophobic peptide, and a neutral pH  $\text{Fe}^{2+}$  wash, to fully reconstitute the metalloprotein complex and maximize the surface positive charge. The layer-by-layer assembly led to changes in the conductivity of the surface, which could readily be followed by cyclic voltammetry in the presence of the redox probe couple  $\text{K}_3\text{Fe}(\text{CN})_6/\text{K}_4\text{Fe}(\text{CN})_6$ . (Figure 1). The reversible redox response of the probe classically obtained on bare gold (not shown) was blocked by formation of alkanethiol SAMs composed of carboxylate and hydroxyl terminal groups on the surface. The sigmoidal behavior between 0.25–0.50 V could be indicative of pinhole defects. Addition of PDEA to the surface caused recovery of the CV signal, owing to the net positive charge of the pyridinium group on PDEA at pH 7.0, which favors association of the negatively charged redox probe with the layer.<sup>20</sup> In contrast, with the positively charged redox probe  $\text{Ru}(\text{NH}_3)_6\text{Cl}_3$ , the redox response after SAMs formation decreased very slightly compared to CV signals on bare gold, and the addition of PDEA to the surface resulted in a significant decrease of redox response (data not shown). The CV signal in the presence of  $\text{K}_3\text{Fe}(\text{CN})_6/\text{K}_4\text{Fe}(\text{CN})_6$  was reduced upon  $[\text{Fe}(\text{envC})_3]^{2+}$  tethering compared to the PDEA coated surface but increased after cysteine and  $\text{Fe}^{2+}$  washes. Tethering of C18-Aib did not incur an ion channel effect, and no CV signal was observed with  $\text{K}_3\text{Fe}(\text{CN})_6/\text{K}_4\text{Fe}(\text{CN})_6$  on a C18-Aib biosensor. The  $[\text{Fe}(\text{envC})_3]^{2+}$  sensor showed no redox activity in the absence of redox marker ions.

The biosensors follow the expected behavior of an ion channel sensor consisting of a protein layer adsorbed on an electrode.<sup>21</sup> At the neutral pH of the experiment, the  $[\text{Fe}(\text{envC})_3]^{2+}$  layer is positively charged, regardless of bound ferrous ion, because of

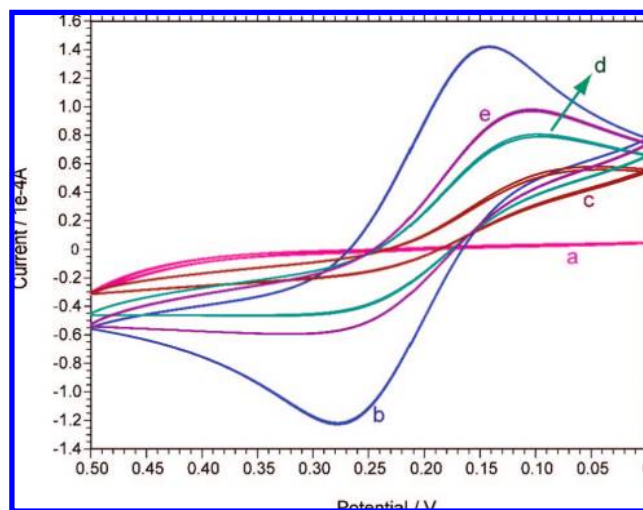


**Figure 1.** Layer-by-layer assembly of a gp41 coiled coil metalloprotein complex  $[\text{Fe}(\text{envC})_3]^{2+}$  on a gold-plated quartz crystal, measured by cyclic voltammetry (CV). Cyclic voltammograms were measured after (a) alkanethiol monolayer formation using 1:1 11-mercaptoundecanoic acid and 6-mercapto-1-hexanol, (b) PDEA coupling, (c)  $[\text{Fe}(\text{envC})_3]^{2+}$  coupling, (d) low pH cysteine wash, (e)  $\text{Fe}(\text{NH}_4)_2(\text{SO}_4)_2$  wash in ultrapure water. For details, see Materials and Methods. CV scans were carried out in 2 mL of 25 mM Tris-acetate buffer solution (100 mM NaCl, pH 7.0) in the presence of 2 mM  $\text{K}_3\text{Fe}(\text{CN})_6$  and 2 mM  $\text{K}_4\text{Fe}(\text{CN})_6$ . The potential was cycled between 0–0.5 V at a rate of  $100 \text{ mV s}^{-1}$ .

the high  $pI$  of the protein (estimated at 8.23<sup>33</sup>). Marker ions accumulate on the charged protein surface, and electron shuttling through pores between adjacent proteins occurs.<sup>21</sup> The effect is enhanced by the positively charged bound ferrous ion. Conversely, C18-Aib is negatively charged at neutral pH ( $pI \approx 4.14$ <sup>34</sup>), and electrostatic repulsion of  $[\text{Fe}(\text{CN})_6]^{3-/4-}$  prevents the accumulation of surface-confined marker ions, a necessary prerequisite to observation of current.<sup>21</sup>

(33) Gasteiger, E.; Hoogland, C.; Gattiker, A.; Duvaud, S.; Wilkins, M. R.; Appel, R. D.; Bairoch, A. In *The Proteomics Protocol Handbook*; Walker, J. M., Ed.; Humana Press: Totowa, NJ, 2005; pp 571–607.

(34) Gasteiger, E.; Gattiker, A.; Hoogland, C.; Ivanyi, I.; Appel, R. D.; Bairoch, A. *Nucleic Acids Res.* **2003**, *31*, 3784–8.

(32) Ayala, C.; Roquet, F.; Valera, L.; Granier, C.; Nicu, L.; Pugniere, M. *Biosens. Bioelectron.* **2007**, *22*, 3113–9.



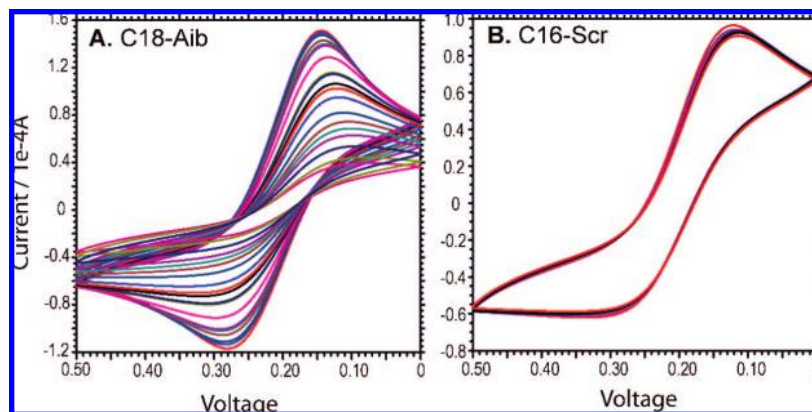


**Figure 2.** CV response of the ion channel biosensor with  $[\text{Fe}(\text{envC})_3]^{2+}$  as the bioreceptor to (A) specific analyte C18-Aib over the concentration range 0–3  $\mu\text{M}$ ; (B) nonspecific analyte C16-Scr over the concentration range 0–5  $\mu\text{M}$ . In part A, the signal decreases with increasing [C18-Aib]. CV scans were measured as described in the caption to Figure 1.

**Response of Electrochemical  $[\text{Fe}(\text{envC})_3]^{2+}$  Biosensor to Analytes.** The  $[\text{Fe}(\text{envC})_3]^{2+}$  biosensor was designed with the hydrophobic pocket midway down the length of a vertically oriented coiled coil, so that specific inhibitors can potentially block the electron conduction pathways between adjacent proteins. Response of the  $[\text{Fe}(\text{envC})_3]^{2+}$  biosensor to specific inhibitors was tested by application of increasing concentrations of a known peptide binding partner C18-Aib and a known nonbinder, the scrambled peptide C16-Scr, as shown in Figure 2. Upon addition of the specific analyte C18-Aib, a stepwise decrease of the observed current through the  $[\text{Fe}(\text{envC})_3]^{2+}$  chip was observed, indicating that the analyte impeded the channeling of electrons to and from the electrode by binding onto the bioreceptor on the chip (Figure 2A). However, the nonspecific analyte C16-Scr failed to elicit a CV response, with virtually no change to the CV signal over a wide range of concentrations (Figure 2B). We observed variable maximum current for different chips (e.g., see Figure 2), which was attributed to the effect of slight differences in the microscopic gold surface or in chip preparation on the channels between adsorbed proteins, to which the ICS is extremely sensitive.<sup>21</sup> Maximum current between chips varied from 60 to 150  $\mu\text{A}$ , as shown in the Supporting Information (Figure S2), which presents the original experimental traces for all analytes measured. The relative change in response with analyte was found to be consistent between chips.

Since the analyte C18-Aib is negatively charged at neutral pH and C16-Scr is almost neutral ( $pI \approx 6.25$ ), it was necessary to test the impact of analyte charge on the signal modulation and the specificity and selectivity of the ICS for gp41 inhibitors. This was achieved by testing additional peptides as well as small molecules known to bind to the hydrophobic pocket, together with some known nonbinders. All had been previously screened in a fluorescence binding assay.<sup>17</sup> The positive controls, in addition to peptide C18-Aib, included ADS-J1, a known small molecule hydrophobic pocket binder,<sup>35</sup> and 11{6,11} and 11{3,5}, two peptidomimetic small molecule inhibitors recently discovered in our laboratory. The negative controls included an additional scrambled peptide C18-Scr, a peptide in which all hydrophobic groups were replaced by Ala (C16-Ala), and the small molecule

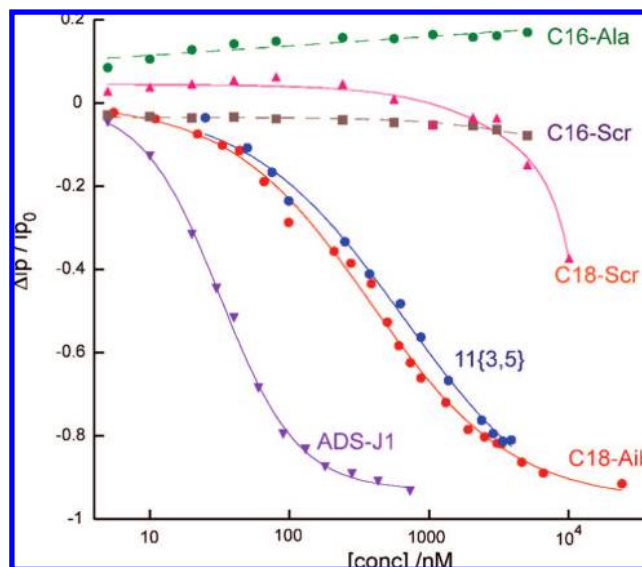


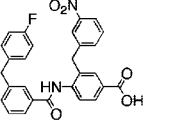
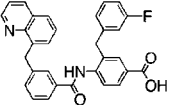
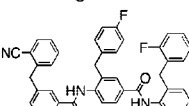
**Figure 3.** CV titration of several peptides and small molecules with the ion channel biosensor using  $[\text{Fe}(\text{envC})_3]^{2+}$ . Sequences or structure of the analytes are given in Table 1. CV experimental parameters were as described in Figure 1. Cathodic peak current was measured, and was normalized to display the fractional change with addition of analyte. Analytes tested were (green ●) C16-Ala, (pink ▲) C18-Scr, (brown ■) C16-Scr, (red ●) C18-Aib, (purple ▼) ADS-J1, (blue ●) 11{3,5}.  $\text{IC}_{50}$  values were obtained by fitting the data to eq 1 using Kaleidagraph.

peptidomimetic compound 12{7,6,4} which gave a false positive reading in the fluorescence experiment.

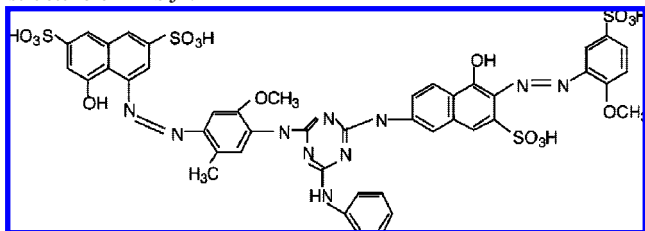
Concentration dependent responses for these analytes were measured by CV, and the results are shown in Figure 3 and Table 1. A clear distinction in biosensor response was observed between positive and negative controls. Importantly, among the series of peptides, only C18-Aib gave a positive response, while scrambled and alanine substituted peptides were negative. One of the scrambled peptides, C18-Scr, has the same  $pI$  as C18-Aib but did not generate a response except at high concentration ( $>5 \mu\text{M}$ ). This observation is attributed to nonspecific hydrophobic binding to the receptor. In the case of hydrophobic peptide analytes which might have a tendency to aggregate or bind nonspecifically, the ICS should be operated at submicromolar analyte concentrations to get a specific response. Of the small molecules 11{6,11}, 11{3,5},

(35) Naicker, K. P.; Jiang, S.; Lu, H.; Ni, J.; Boyer-Chatenet, L.; Wang, L.-X.; Debnath, A. K. *Bioorg. Med. Chem.* **2004**, *12*, 1215–20.

**Table 1. Peptide Sequences, Compound Structures and IC<sub>50</sub> Observed by ICS, Compared to Fluorescence-Detected Inhibition Constants, K<sub>i</sub><sup>a</sup>**

Analyte	Sequence / structure	pI / pK <sub>a</sub> <sup>†</sup>	MWt	IC <sub>50</sub> (μM) (ICS)	K <sub>i</sub> (μM) (fluorescence)
C16-Scr	DYETMIKWEIWK-KRC	6.25	2158.5	-	-
C18-Scr	MMIWNTDEILTNE-SYRWC	4.14	2305.6	> 10	-
C16-Ala	AMEAARKAEET-KKAC	8.22	1708	-	-
C18-Aib	MTWBEWDREIBN-YTSLIC	4.14	2271.1	0.38 ± 0.05	0.8 ± 0.13
ADS-J1	*	≤1.5 <sup>a</sup>	1177	0.032 ± 0.008	0.35 ± 0.09
11{6,11}		3.87	484.5	0.31 ± 0.10	1.3 ± 0.2
11{3,5}		3.93	490.5	0.66 ± 0.14	1.5 ± 0.2
12{7,6,4}		neutral	573.6	-	false positive

<sup>a</sup> K<sub>i</sub> from ref 17; dashed lines indicate no binding observed; peptide pI calculated from ExPASy;<sup>33</sup> compound pK<sub>a</sub> calculated using SPARC;<sup>47</sup> <sup>a</sup>, estimated from pK<sub>a</sub> of 2-hydroxy-6-naphthalene sulfonic acid;<sup>48</sup> \*, structure of ADS-J1:



and 12(7,6,4), only the first two gave a positive response. 12(7,6,4) was detected as a false positive in the fluorescence experiment due to interaction between the compound and the fluorescent probe. Any true binding propensity of 12(7,6,4) to the hydrophobic pocket would have been hidden from detection by the fluorescence method but does not appear to occur.

The data in Figure 3 was fit to obtain IC<sub>50</sub> values according to the equation

$$\Delta i_p / i_{p_0} = -c / (1 + (IC_{50} / A_p)^n) \quad (1)$$

$i_p$  is the cathodic peak current recorded at analyte concentration  $A_p$ ,  $i_{p_0}$  is the current in the absence of analyte, and  $\Delta i_p = i_p - i_{p_0}$ .  $c$  is a constant representing the dynamic range of the measurement (close to -1), and  $n$  is the Hill slope. The IC<sub>50</sub> values obtained are compared with K<sub>i</sub> values determined from the fluorescence experiment in Table 1; the very low receptor concentration ( $10^{11}$ – $10^{12}$  molecules on the surface) would imply that the IC<sub>50</sub> should be equal to the K<sub>i</sub>.<sup>36</sup> However, for all four specific inhibitors, the IC<sub>50</sub> was found to be less than the K<sub>i</sub>, by a

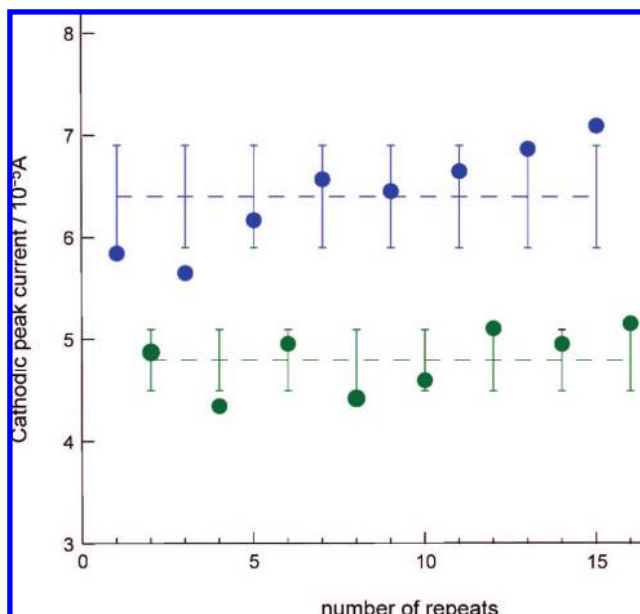


**Figure 4.** Repeat measurements and chip regeneration. Sixteen measurements of the CV on an [Fe(envC)<sub>3</sub>]<sup>2+</sup> functionalized chip with successive application of 30 nM ADS-J1 (green ●) and 0.125% SDS (blue ●). The error bars represent the standard deviation of the data points from the mean, which is shown as a dashed horizontal line.

factor of 2–3 for three of the inhibitors, and a factor of 10 for ADS-J1. All of the inhibitors are negatively charged at neutral pH, and the effect of analyte charge on the response must be considered.<sup>21</sup> For a negatively charged analyte, suppression of marker ion currents occurs both by occlusion of the pores due to specific binding and by reduction of the positive charge of the protein layer and hence the concentration of marker ions associated with the surface. Consequently, the most highly charged analyte, ADS-J1, exhibits the greatest deviation from solution K<sub>i</sub> and the highest cooperativity of binding, with a Hill slope of 1.56 (Supporting Information).

**Regeneration of the ICS.** Regeneration and reuse of the ion channel biosensor was tested by several rounds of application of a solution of 30 nM ADS-J1 followed by 0.125% sodium dodecyl sulfate, as shown in Figure 4. The response remained consistent over eight repetitions, with cathodic peak currents of  $48 \pm 3$  and  $64 \pm 5$  μA for the biosensor in the presence of analyte and after regeneration, respectively. We have not reused or tested the chips past eight cycles. The biosensor was found to be stable for extended periods at 4 °C and over a voltage sweep range of 0–0.5 V.<sup>37</sup>

**Confirmation of Bioreceptor Activity by SPR.** SPR measurements were used to confirm biosensor preparation and activity. The analogous chip assembly process was followed from the SPR response (Supporting Information, Table S1), and analyte responses were tested for both the [Fe(envC)<sub>3</sub>]<sup>2+</sup> and C18-Aib functionalized chips (Supporting Information, Figure S1). SPR results yielded K<sub>d</sub>'s of approximately 10 and 4 μM for the ligand–analyte interactions [Fe(envC)<sub>3</sub>]<sup>2+</sup>–C18-Aib and C18-Aib–[Fe(env2.0)<sub>3</sub>]<sup>2+</sup>, respectively. SPR results were used mainly to ascertain activity of immobilized bioreceptor. Quantitative analysis can be inaccurate due to the difficulties inherent in

(36) Cheng, Y.; Prusoff, W. H. *Biochem. Pharmacol.* **1973**, *22*, 3099–108.

(37) Everett, W. R.; Fritsch-Faules, I. *Anal. Chim. Acta* **1995**, *307*, 253–68.

measuring low-affinity interactions by SPR when maximum analyte concentration is limited or causes hydrophobic aggregation.<sup>38–40,41,42,43,44,45,46</sup>

**Comparison of Affinity Measurements by Different Techniques.** There are important distinguishing features between solution- and surface-based detection of inhibitor binding. These include the range of inhibitor affinities and concentrations accessible by the different techniques, the sensitivity and accuracy of each method, and the mode of detection, i.e., competitive inhibition vs direct detection. The low receptor concentration required to form the ICS resulted in sensitivity to high-affinity binders with  $IC_{50}$ 's in the low nanomolar to low micromolar range. Consequently, the sensor could detect analytes with concentrations of 10–1000 nM. This is complementary to the fluorescence assay which can measure inhibitors with  $10^{-1}$ – $10^2$   $\mu$ M  $K_i$ 's and which requires 10–50  $\mu$ M inhibitor concentrations.<sup>17</sup>

The ion channel biosensor measures analyte binding in a direct way, rather than by competitive inhibition, and no labeled C-peptide binding partner is required as in the fluorescence experiment. As demonstrated above, the affinity of negatively charged analytes was overestimated by a factor that appeared to correlate with analyte  $pI$  or  $pK_a$ . The interaction of inhibitors in the gp41 hydrophobic pocket involves both hydrophobic and electrostatic contacts,<sup>38,40</sup> and the charge on the inhibitors plays a crucial role in binding.<sup>41,42</sup> It is impossible to avoid the effect of analyte charge on the ICS response.<sup>21</sup> We have shown that specific structural interactions are important for determining ICS specificity and that charge alone is not a sufficient criterion for observation of a response. A negatively charged peptide of the incorrect sequence tests negative. Reasonable values for inhibitor affinity and consistent rank ordering were obtained for partially charged analytes. The discrepancy was larger in the case of a highly charged analyte. With the ICS response tested with a wider variety of peptides and small molecules with differing charges, the charge contribution to the response may be elucidated. This is the subject of future work.

Low-molecular weight inhibitors can be detected efficiently by ICS compared to SPR, in which accuracy of the detection is generally limited in the case of sensing small molecules. Furthermore, nonspecific hydrophobic associations make SPR measure-

ment of response at saturation difficult. Maximum response as a function of analyte concentration is necessary for SPR quantification of a micromolar association. Failure to measure the maximum response can lead to inaccuracies in assessed  $K_d$ 's. In the ICS, it is easier to estimate the maximum response, which should be close to zero current ( $\Delta i_p/i_{p0} = -1$ ).

## CONCLUSIONS

In summary, we have demonstrated an ion channel biosensor for detection of HIV-1 gp41 inhibitors using electrochemical signal transduction. The sensor was constructed from a section of the gp41 coiled coil domain corresponding to the hydrophobic pocket region and stabilized in its trimeric form by a metal ion. It was shown to respond specifically to peptides and inhibitors known to bind in the hydrophobic pocket, with a resulting decrease in the current observed in the presence of the redox probe  $[Fe(CN)_6]^{3-/4-}$ . The current change was caused by inhibitor blocking of the artificial ion channels created by the positively charged metalloprotein coiled coil arrayed on the sensor surface. Channel blocking was enhanced by the negative charge of coiled coil binders, leading to enhanced apparent affinity as measured by ICS. Inhibitors of approximately equivalent charge could be rank-ordered according to their relative affinities.

Detection of low-molecular weight inhibitors and C-peptides which bind to the N-terminal coiled coil of several class 1 viral fusion domains has been shown to be an effective strategy for identifying viral fusion inhibitors.<sup>6</sup> In many class 1 viruses, the C-peptide is ill-defined in the postfusion conformation, either due to extended strand structure for the C-terminal domain<sup>43,44</sup> or an unknown three-dimensional structure. On the other hand, the coiled coil domain is usually recognizable from sequence analysis.<sup>45,46</sup> The present biosensor assay which measures direct binding on the coiled coil does not require identification of the C-terminal peptide domain, offering a promising application for extending the assay to a variety of class 1 viral fusion domains.

## ACKNOWLEDGMENT

We thank Dr. Peter Hwang, University of California San Francisco, for access and training in the use of the Biacore 1000 and for invaluable discussions. This work was supported by University-wide AIDS Research Grant (California HIV/AIDS Research Program) Grant ID05-TOURO-041. Additional support was provided by Touro University.

## SUPPORTING INFORMATION AVAILABLE

SPR chip preparation details, and table and figure of SPR data, plus experimental CV traces and parameters from fitting ICS dose response data (Table 1 and Figure 3) to eq 1. This material is available free of charge via the Internet at <http://pubs.acs.org>.

Received for review March 11, 2008. Accepted May 31, 2008.

AC800511N

- (38) Cole, J. L.; Garsky, V. M. *Biochemistry* **2001**, *40*, 5633–41.
- (39) Jiang, S.; Debnath, A. K. *Biochem. Biophys. Res. Commun.* **2000**, *270*, 153–7.
- (40) Strockbine, B.; Rizzo, R. C. *Proteins* **2007**, *67*, 630–42.
- (41) Ernst, J. T.; Kutzki, O.; Debnath, A. K.; Jiang, S.; Lu, H.; Hamilton, A. D. *Angew. Chem., Int. Ed.* **2002**, *41*, 278–81.
- (42) Jiang, S.; Lu, H.; Liu, S.; Zhao, Q.; He, Y.; Debnath, A. K. *Antimicrob. Agents Chemother.* **2004**, *48*, 4349–59.
- (43) Kobe, B.; Center, R. J.; Kemp, B. E.; Poumbourios, P. *Proc. Natl. Acad. Sci. U.S.A.* **1999**, *96*, 4319–24.
- (44) Park, H. E.; Gruenke, J. A.; White, J. M. *Nat. Struct. Biol.* **2003**, *10*, 1048–53.
- (45) Singh, M.; Berger, B.; Kim, P. S. *J. Mol. Biol.* **1999**, *290*, 1031–41.
- (46) Singh, M.; Berger, B.; Kim, P. S.; Berger, J. M.; Cochran, A. G. *Proc. Natl. Acad. Sci. U.S.A.* **1998**, *95*, 2738–43.
- (47) Hilal, S. H.; Karickhoff, S. W.; Carreira, L. A. *Quant. Struct.-Act. Relat.* **1995**, *14*, 348.
- (48) Engel, K. H.; Hutchison, A. W. *J. Am. Chem. Soc.* **1930**, *52*, 211–216.